



HAL
open science

In vivo multiphoton microscopy shows that a single 10 nanosecond pulsed electric field is sufficient to disrupt vasculature in xenografted human glioblastoma spheroids

Sylvia M. Bardet, Lynn Carr, Malak Soueid, Delia Arnaud-Cormos, Philippe Lévêque, Rodney Philip O'Connor

► **To cite this version:**

Sylvia M. Bardet, Lynn Carr, Malak Soueid, Delia Arnaud-Cormos, Philippe Lévêque, et al.. In vivo multiphoton microscopy shows that a single 10 nanosecond pulsed electric field is sufficient to disrupt vasculature in xenografted human glioblastoma spheroids. BioEM2015, Joint Meeting of the BioElectroMagnetics Society and the European BioElectromagnetics Association, BEMS & EBEA, Jun 2015, Pacific Grove, CA, United States. hal-02469279

HAL Id: hal-02469279

<https://hal.science/hal-02469279>

Submitted on 14 Feb 2020

HAL is a multi-disciplinary open access archive for the deposit and dissemination of scientific research documents, whether they are published or not. The documents may come from teaching and research institutions in France or abroad, or from public or private research centers.

L'archive ouverte pluridisciplinaire **HAL**, est destinée au dépôt et à la diffusion de documents scientifiques de niveau recherche, publiés ou non, émanant des établissements d'enseignement et de recherche français ou étrangers, des laboratoires publics ou privés.

PA-145 [19:00]

In vivo multiphoton microscopy shows that a single 10 nanosecond pulsed electric field is sufficient to disrupt vasculature in xenografted human glioblastoma

Sylvia M. Bardet¹, Lynn Carr¹, Malak Soueid², Delia Arnaud-Cormos², Philippe Leveque² & Rodney P. O'Connor¹

¹BioEPIX, LabEx Sigma-Lim, XLIM, LIMOGES, France, 87060

²XLIM, CNRS UMR 7252, LIMOGES, France, 87060

Keywords: In vivo, Pulsed, Completed (unpublished)

Here we present an *in vivo* exposure system for studying the influence of nanosecond pulsed electric fields (nsPEFs) on tumour microenvironment using multiphoton imaging. We found that a single nsPEF (10ns, 30-50kV/cm) strongly affects the tumour neovascular network, collapsing micro-capillaries irreversibly but transiently affecting the diameter of larger vessels. Human glioblastoma cells (U87-MG) grafted into the avian chorioallantoic membrane (CAM) were immediately depleted of their blood supplies, showing the early events of nsPEF effects in a complex tissue environment with multiphoton intravital imaging.

Introduction

High-intensity pulsed electric fields with nanosecond durations (3-300ns; nsPEFs) have emerged as a promising tool for tumor ablation [1,2,3]. The physical mechanisms and specific type of cell death that occurs following the application of nsPEFs is under investigation by several groups and initial studies have shown effects on cell signaling through calcium and cell death pathways [4,5,6], mitochondria [7] and cytoskeleton [8,9,10].

In order to understand the utility of nsPEF in treating solid and resistant cancer, we developed a system to apply electromagnetic fields *in vivo* to vascularized 3D tumours, similar to the one used for longer pulse duration (50 μ m) in canine patient [11]. We used multiphoton microscopy tools and intravital imaging to study how nsPEFs affect tumor cell physiology and microenvironment by xenografting human cancer cells into the avian chorioallantoic membrane (CAM), allowing the study of the response at the level of tumor microenvironment *in vivo*, where tumor cells are vascularized and proliferating in 3 dimensions.

Methods

1. In vivo model

Shell-less ex ovo chorioallantoic membranes (CAM) from quail eggs were grafted with human U87-MG glioblastoma cells (ATCC® HTB-14™) that were modified by lentiviral infection to stably express fLuc2 and GFP (U87-fLuc2/GFP, maximum excitation λ =395nm, maximum emission λ =509nm) under the control of the CMV. Embryos were maintained in the incubator until tumor size reached 0.5-1mm in diameter and had clear vascularization, usually 48h post-implantation.

2. Exposure system

We developed an nsPEF exposure setup (Fig.1), composed of an nsPEF generator, a digital phosphor oscilloscope (DPO), a high-voltage measurement device (tap-off), an electrode-based delivery system and a microscope stage. The nsPEF generator (FPG 10-INM-T, FID Technology, Germany) delivered 10ns pulses with amplitudes between 4.5kV and 10kV and with rise-times around 5ns. A 1GHz oscilloscope (DPO 4104, Tektronix, USA) using 30dB attenuator connected to the 40dB attenuation tap-off was used to display the time-domain measurements of each delivered electrical pulse. The numerical dosimetry of the nsPEF exposure setup was performed using numerical modeling and full-wave 3D simulations based on a discretization of Maxwell's equations in integral form [12,13].

3. 3D time-lapse fluorescence measurements

Embryos were positioned on a heated microscope stage of a customized Olympus multiphoton microscope BX61WI/FV1200MPE with a 25X immersion objective (1.05NA, 2.0mm working distance) coupled with a tunable femtosecond Ti:Sapphire pulsed laser (Chameleon Ultra II, Coherent) for the excitation. The nsPEF delivery electrodes were positioned alongside tumours at the CAM surface with a micromanipulator under the microscope objective. To visualize the blood flow, Rhodamine B isothiocyanate Dextran 70kDa was injected in the peripheral vasculature of the CAM. Image stacks were taken at 2 μ m steps, acquired under 870nm excitation wavelength each 5min with FluoView FV1200 software (v4.1.1.5, Olympus). The different components of the emitted light from the sample were separated using a dichroic mirror (570nm) and detected by a pair of photomultiplier tubes preceded by fluorophore specific emission filters (BA 575-630 for Rhodamine, BA 495-540 for GFP).

The images obtained were analyzed with Imaris software (Bitplane AG) or Fiji/ImageJ (NIH), which were used to background correct and median filter all images equally across treated samples and controls.

Results

The dosimetry of the *in vivo* delivery system showed that the electric field in the central region between the electrodes had a good homogeneity, as based on 3D numerical simulations (Fig.1b). The intensity of the electric field delivered to the tumour in this central region was between 30-50 kV/cm.

Consistent with previous results [2], we observed a strong effect of nsPEF on tumour vasculature. Relative blood volume ($\Delta V/V_0$) and blood fluorescence ($\Delta F/F_0$) measurements were performed on Z-stacks of vascularized tumours and peripheral CAM networks. The application of a single 10ns PEF drastically affected blood flow, which decreased progressively to 20% inside the tumor, but that also was accompanied by bleeding and an increase in extravascular fluorescence volume (287.52%) and fluorescence (387.10%), immediately after treatment and continuing at $t=20\text{min}$ (Fig.2). We demonstrated that the application of a single nsPEF application had a greater impact on capillaries and smaller neovasculature, than on the larger vessels of the CAM.

Conclusion

We have developed and characterized a new system for studying the effects of nsPEF in vivo using intravital multiphoton imaging of tumours expressing fluorescent protein reporters. This approach provides real-time information about the early events in tumour microenvironment that occur after nsPEF treatment. A disruption of neovasculature was visualized following the application of a single nsPEF, similar to that previously observed with Doppler ultrasound and histology [2,14,15,16]. The vascular effects of nsPEFs are comparable to those seen with pulses of longer duration (100 μs) in mouse skin [17], in mouse hindlimb muscle [18] or rabbit organs [19], suggesting a general effect of electrical stimulation on tissue perfusion that extends to the nanosecond regime. The predominance of the observed effect on capillaries and absence of innervation in the CAM vasculature allows us to rule out neurovascular mechanisms and points to direct effects of nsPEFs on endothelia and cytoskeleton at their junctions [20]. The subcellular resolution of multiphoton microscopy allows us to directly image this in future studies. In summary, we have shown a robust effect of a single 10ns PEF on vascularized glioblastoma in 3D, highlighting the importance of vessel size and morphology in these effects and resolving these responses in time. Future work will combine fluorescent and bioluminescent reporters to measure tumour regression and to visualize the signaling pathways activated in vivo in the hours and days following nsPEF application.

References

1. Chen, X., Zhuang, J., Kolb, J. F., Schoenbach, K. H., and Beebe, S. J. (2012). "Long term survival of mice with hepatocellular carcinoma after pulse power ablation with nanosecond pulsed electric fields." *Technol Cancer Res Treat* 11(1): 83-93.
2. Nuccitelli, R., Pliquett, U., Chen, X., Ford, W., James Swanson, R., Beebe, S. J., Kolb, J. F., and Schoenbach, K. H. (2006). "Nanosecond pulsed electric fields cause melanomas to self-destruct." *Biochem Biophys Res Commun* 343(2): 351-360.
3. Chen, X. H., Beebe, S. J., and Zheng, S. S. (2012). "Tumor ablation with nanosecond pulsed electric fields." *Hepatobiliary Pancreat Dis Int* 11(2): 122-124.
4. Zhang, J., Blackmore, P. F., Hargrave, B. Y., Xiao, S., Beebe, S. J., and Schoenbach, K. H. (2008). "Nanosecond pulse electric field (nanopulse): a novel non-ligand agonist for platelet activation." *Arch Biochem Biophys* 471(2): 240-248.
5. Morotomi-Yano, K., Akiyama, H., and Yano, K. (2014). "Different involvement of extracellular calcium in two modes of cell death induced by nanosecond pulsed electric fields." *Arch Biochem Biophys* 555-556: 47-54.
6. Pakhomova, O. N., Gregory, B., Semenov, I., and Pakhomov, A. G. (2014). "Calcium-mediated pore expansion and cell death following nanoelectroporation." *Biochim Biophys Acta* 1838(10): 2547-2554.
7. Beebe, S. J., Sain, N. M., and Ren, W. (2013). "Induction of Cell Death Mechanisms and Apoptosis by Nanosecond Pulsed Electric Fields (nsPEFs)." *Cells* 2(1): 136-162.
8. Thompson, G. L., Roth, C. C., Dalzell, D. R., Kuipers, M., and Ibey, B. L. (2014). "Calcium influx affects intracellular transport and membrane repair following nanosecond pulsed electric field exposure." *J Biomed Opt* 19(5): 055005.
9. Rassokhin, M. A. and A. G. Pakhomov (2014). "Cellular regulation of extension and retraction of pseudopod-like blebs produced by nanosecond pulsed electric field (nsPEF)." *Cell Biochem Biophys* 69(3): 555-566.
10. Pakhomov, A. G., Xiao, S., Pakhomova, O. N., Semenov, I., Kuipers, M. A., and Ibey, B. L. (2014). "Disassembly of actin structures by nanosecond pulsed electric field is a downstream effect of cell swelling." *Bioelectrochemistry* 100:88-95.
11. Garcia, P. A., Pancotto, T., Rossmeisl, J. H., Jr., Henao-Guerrero, N., Gustafson, N. R., Daniel, G. B., Robertson, J. L., Ellis, T. L., and Davalos, R. V. (2011). "Non-thermal irreversible electroporation (N-TIRE) and adjuvant fractionated radiotherapeutic multimodal therapy for intracranial malignant glioma in a canine patient." *Technol Cancer Res Treat* 10(1): 73-83.
12. Kanaan, M., El Amari, S., Silve, A., Merla, C., Mir, L. M., Couderc, V., Arnaud-Cormos, D. and Leveque, P. (2011). "Characterization of a 50- Ω Exposure Setup for High-Voltage Nanosecond Pulsed Electric Field Bioexperiments." *Biomedical Engineering, IEEE Transactions* 58(1): 207-214.
13. Wu, Y. H., Arnaud-Cormos, D., Casciola, M., Sanders, J. M., Leveque, P., Vernier, P. T. (2013). "Moveable Wire Electrode Microchamber for Nanosecond Pulsed Electric-Field Delivery." *Biomedical Engineering, IEEE Transactions* 60(2): 489-496.
14. Nuccitelli, R., Chen, X., Pakhomov, A. G., Baldwin, W. H., Sheikh, S., Pomicter, J. L., Ren, W., Osgood, C., Swanson, R. J., Kolb, J. F., Beebe, S. J., and Schoenbach, K. H. (2009). "A new pulsed electric field therapy for melanoma disrupts the tumor's blood supply and causes complete remission without recurrence." *Int J Cancer* 125(2): 438-445.
15. Sersa, G., Jarm, T., Kotnik, T., Coer, A., Podkrajsek, M., Sentjerc, M., Miklavcic, D., Kadivec, M., Kranjc, S., Secerov, A.,

- and Cemazar, M. (2008). "Vascular disrupting action of electroporation and electrochemotherapy with bleomycin in murine sarcoma." *Br J Cancer* 98(2): 388-398.
16. Jarm, T., Cemazar, M., Miklavcic, D., and Sersa, G. Jarm, T., et al. (2010). "Antivascular effects of electrochemotherapy: implications in treatment of bleeding metastases." *Expert Rev Anticancer Ther* 10(5): 729-746.
17. Bellard, E., Markelc, B., Pelofy, S., Le Guerroue, F., Sersa, G., Teissie, J., Cemazar, M., and Golzio, M. (2012). "Intravital microscopy at the single vessel level brings new insights of vascular modification mechanisms induced by electropermeabilization." *J Control Release* 163(3): 396-403.
18. Gehl, J., Skovsgaard, T., and Mir, L. M. (2002). "Vascular reactions to in vivo electroporation: characterization and consequences for drug and gene delivery." *Biochim Biophys Acta* 1569(1-3): 51-58.
19. Ramirez, L. H., Orłowski, S., An, D., Bindoula, G., Dzodic, R., Ardouin, P., Bognel, C., Belehradec, J., Jr., Munck, J. N., Mir, L. (1998). "Electrochemotherapy on liver tumours in rabbits." *Br J Cancer* 77(12):2104-11.
20. Kanthou, C., Kranjc, S., Sersa, G., Tozer, G., Zupanic, A., and Cemazar, M. Kanthou, C., et al. (2006). "The endothelial cytoskeleton as a target of electroporation-based therapies." *Mol Cancer Ther* 5(12): 3145-3152.

Figures

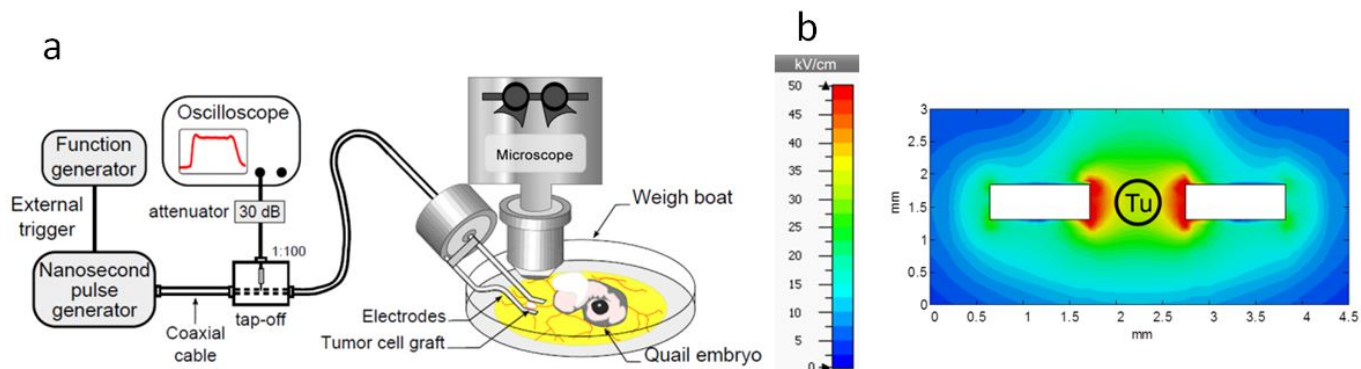


Figure 1. nsPEF exposure setup. a) Nanosecond pulse generator, measurement device (oscilloscope) and microscope stage, b) Spatial distribution of the electric field magnitude of the delivery system around the tumor (Tu) for a 6.1-kV delivered voltage in a 2D vertical plane perpendicular to the electrode tip.

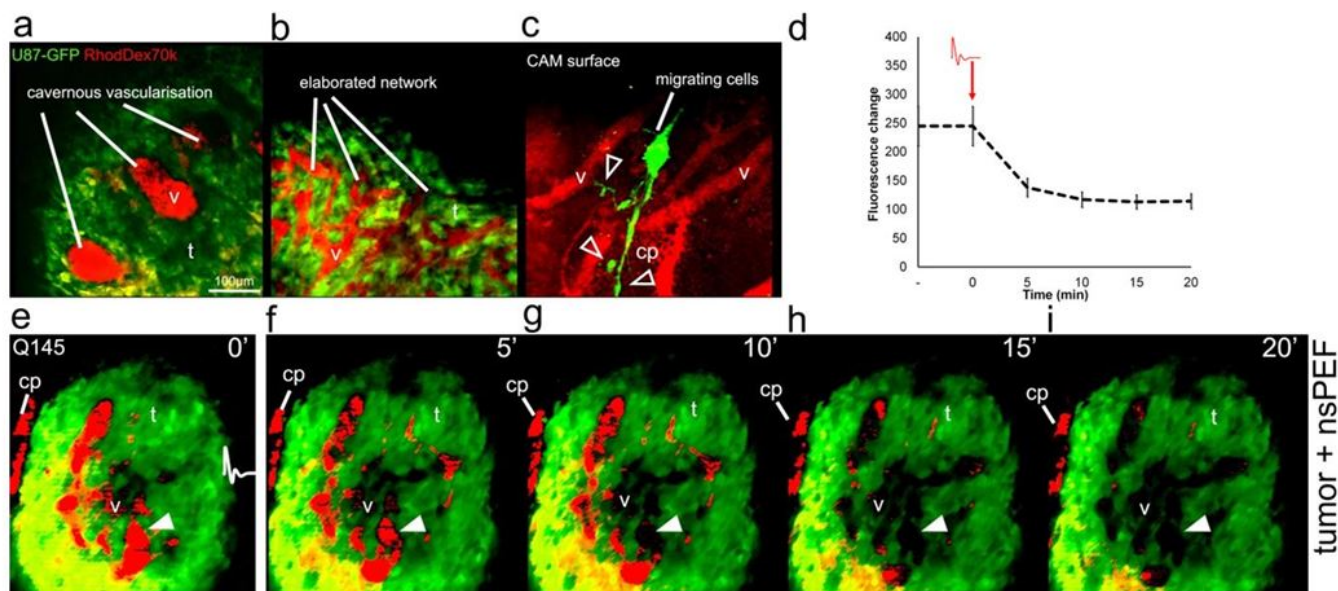


Figure 2. Graft of U87 cells show complex irrigation patterns that can be depressed by nsPEF. Intravascular rhodamine dextran and GFP-U87 grafted on CAM were observed with multiphoton microscope and average Z-stacks are (a-c, e-i). Measurements of fluorescence change relative to blood volume are represented on graph (d) over time before and after nsPEF treatment. v = vessels, t = tumor mass, cp = capillary plexus. Scale bar in (a) = 100µm applied to all.

PA-147 [19:00]

mmWave Exposure Assessment using Magnetic Resonance Thermal Imaging

Leeor Alon^{1, 2, 3}, William S. Slovinsky⁴, Gene Y. Cho^{1, 2}, Daniel K. Sodickson^{1, 2, 3}, Christopher M. Collins^{1, 2, 3}, Marvin Ziskin⁴, Theodore S. Rappaport^{1, 3} & Cem M. Deniz^{1, 2, 3}

¹Department of Radiology, New York University School of Medicine, New York, NY, USA, 10016

²Center for Advanced Imaging Innovation and Research (CAI2R), New York University School of Medicine, New York, NY, USA, 10016